Stimulated supercontinuum generation extends broadening limits in silicon

P. T. S. DeVore,[1,a)] D. R. Solli,[1,2] C. Ropers,[1,2] P. Koonath,[1] and B. Jalali[1,3]
[1]*Department of Electrical Engineering, University of California, Los Angeles, California 90095, USA*
[2]*Courant Research Center Nano-Spectroscopy and X-Ray Imaging, University of Göttingen, Germany*
[3]*California NanoSystems Institute, University of California, Los Angeles, California 90095, USA*

(Received 6 February 2012; accepted 11 February 2012; published online 8 March 2012)

We demonstrate that stimulated supercontinuum generation alleviates restrictions on spectral broadening in silicon waveguides. At telecommunications wavelengths, two-photon and free-carrier absorption typically deplete the pump before large broadening factors can be achieved. However, broadening via modulation instability (MI) can be enhanced by seeding, which also substantially improves the energy efficiency of spectral broadening in media with nonlinear loss. Coherent seeding also generates a stable output spectrum, in contrast to conventional approaches where broadening starts from noise. The combination of self-phase modulation and stimulated modulation instability generates broadening factors in excess of 40-fold at moderate intensity levels, with >15-times better energy efficiency. © *2012 American Institute of Physics*. [http://dx.doi.org/10.1063/1.3692103]

Broadband "white" light known as supercontinuum (SC) radiation[1,2] finds diverse applications in frequency metrology,[3] spectroscopy,[4,5] biophotonics,[6,7] and wavelength-division multiplexing (WDM) communication.[8–10] While nonlinear optical fiber is typically employed to produce this radiation, the generation of broadband light in silicon waveguides has been experimentally and theoretically investigated,[11–14] and is of interest for, e.g., chip-scale sensing applications and future optical interconnects based on WDM.[8,15] Rapid spectral broadening requires an intense pump and a strong optical nonlinearity. Silicon has a strong Kerr nonlinearity, but two-photon absorption (TPA) and free-carrier absorption (FCA)—phenomena that are absent in optical fiber—restrict the broadening factor.[14,16] Furthermore, Raman scattering in silicon has a relatively narrow gain bandwidth and an appreciable frequency shift and, thus, does not play a significant role in broadening the spectrum. Consequently, the broadening factors found in silicon are much smaller than those in optical fiber.

A high-intensity pump pulse in a silicon waveguide modulates the medium's refractive index, leading to self-phase modulation (SPM) of the pulse and, thus, spectral broadening. Both the Kerr nonlinearity and refraction caused by free carriers (FCR) contribute to SPM. The carriers are generated by TPA and tend to accumulate due to their relatively long lifetime. The Kerr effect produces blueshifted frequencies on the pulse's trailing edge and redshifted components on its leading edge, while FCR induces a blueshift throughout the pulse. The net effect is a blueshifted continuum with new frequencies residing predominantly in the pulse's trailing side.[14,17] However, the accumulating carriers substantially attenuate these components. Together with TPA, this process leads to self-limited broadening in the normal dispersion regime.[14]

Broader bandwidths can be realized (but with similar broadening factors) by driving the nonlinear process with ultrashort pump pulses, which also produce fewer free carriers for a fixed power level.[13,18] Anomalous and higher-order dispersion also create the possibility of achieving large bandwidths through modulation instability (MI) (Ref. 19) and soliton fission.[13] However, TPA and FCA tend to dampen MI and inhibit broadening, except in the mid-infrared regime where nonlinear absorption is nearly eliminated.[20]

In this paper, we realize large spectral broadening factors in a silicon waveguide despite the presence of TPA and free-carrier effects. In our simulations, previous spectral broadening limitations are overcome by stimulating MI with a weak seed that jumpstarts the nonlinear interaction. In addition, we show that coherent seeding produces a low noise SC, in contrast to that resulting from noise-driven MI. To motivate further discussion, we show the impact of a weak seed on pulse propagation in a silicon waveguide with anomalous dispersion (cf. Fig. 1). An understanding of this result is facilitated by a brief examination of spectral broadening effects in fiber.

In glass fiber, MI is readily driven by ambient noise at moderate pump power levels, ultimately leading to soliton fission and intra-pulse Raman scattering.[2] While this process can generate huge broadening factors, it typically leads to substantial spectral fluctuations. Real-time measurements have shown that specific input fluctuations can even lead to extreme output statistics and rare events known as optical rogue waves.[21] This finding led to the demonstration of controlled SC seeding, which results in lower input power requirements and a coherent output.[22] Extremely stable stimulated SC can be obtained by deriving the pump and seed from a parametric oscillator,[23] and seeding may even be used to slow the spectral broadening process.[24] Other fiber-based studies have also found benefits of added input modulation.[25–28] In silicon, seeding of SC has recently been used in the mid-infrared (where TPA and FCA are absent) to study the origin of certain spectral features and measure gain,[29] but did not contribute to broadening.

The advantages of stimulated SC generation known in fiber, particularly the reduction in pump power requirements,

a)Author to whom correspondence should be addressed. Electronic mail: pdevore@ucla.edu.

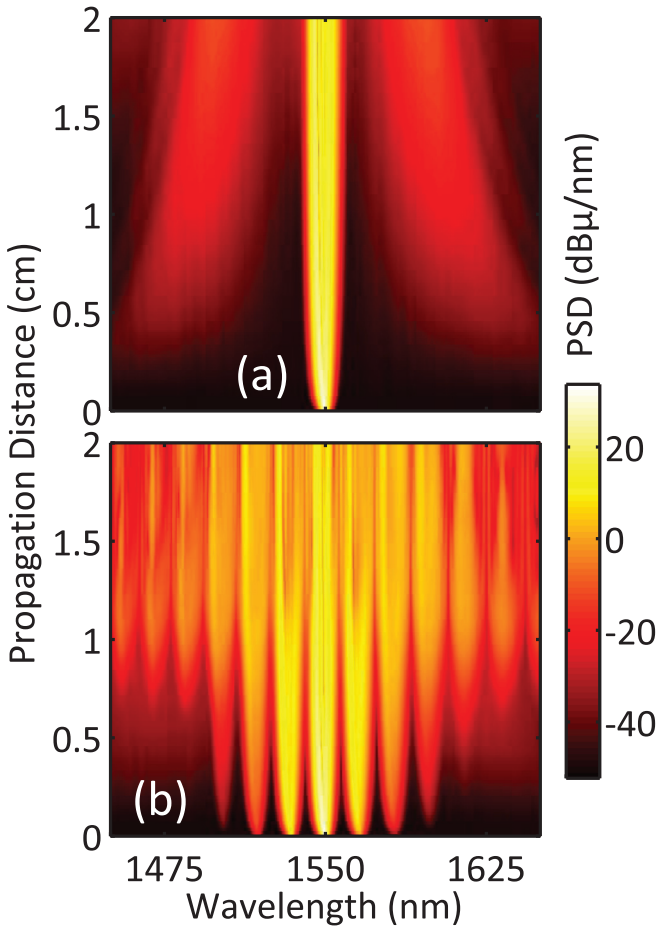

FIG. 1. (Color online) Simulation of picosecond pulse propagation in a silicon waveguide without (a) and with (b) the addition of a weak wavelength-shifted seed pulse. PSD: power spectral density. Pump peak intensity: 10 GW/cm^2; seed peak intensity: 100 MW/cm^2; seed frequency shift: 2 THz; seed timing: −1 ps (precedes pump); leading-order dispersion: $\beta_2 = -2.18$ ps^2/m; input noise of one photon per mode included. Simulation details provided below.

suggest its application to overcome the broadening limitations imposed by TPA and FCA in silicon. Fiber-based results also imply that seeding may facilitate the generation of coherent SC in silicon—an enhancement that could be implemented in both the near- and mid-infrared regimes. We simulate pulse propagation in silicon waveguides using the generalized nonlinear Schrodinger equation,

$$\frac{\partial A(z,t)}{\partial z} = \sum_{k\geq 2} \frac{i^{k+1}}{k!}\beta_k \frac{\partial^k A(z,t)}{\partial t^k} + i\gamma A(z,t)|A(z,t)|^2 - (\alpha_l + \alpha_{FCA}) + \frac{2\pi i}{\lambda_0} n_{FCR},$$

where $A(z,t)$ is the slowly varying envelope, β_k are the wavevector coefficients, γ is the nonlinear coefficient (Kerr and TPA), the linear loss α_l is set to zero (except where noted otherwise), and α_{FCA} and n_{FCR} account for carrier-dependent absorption and refraction.[14,30] Carriers are created by TPA and survive for the duration of the pulse; additional details can be found in Refs. 14 and 17. Raman scattering is included (not shown above),[13] but has only a minor impact. To realize anomalous dispersion, we choose dispersion-engineered silicon-on-insulator (SOI) strip waveguides (air cladding) with cross-sectional dimensions below 1 μm; such waveguides have been shown to allow efficient phase matching for four-wave mixing at telecom wavelengths.[31] Dispersion properties are calculated by independent mode calculations. We present simulations from two different waveguides (2 cm length) with the following dispersive parameters: $\beta_2 = -2.18$ ps^2/m, $\beta_3 = 9.24 \times 10^{-3}$ ps^3/m, $\beta_4 = -2.27 \times 10^{-5}$ ps^4/m (waveguide 1) and $\beta_2 = -0.519$ ps^2/m, $\beta_3 = 5.20 \times 10^{-3}$ ps^3/m, $\beta_4 = -5.70 \times 10^{-6}$ ps^4/m (waveguide 2). Stimulated SC generation is implemented by introducing a weak (20 dB below pump), frequency-shifted (~2–3.5 THz) seed to co-propagate with the pump (3.5 ps transform-limited pulses for pump and seed or quasi-continuous-wave seed of 1 ns). The ideal seed timing is generally ahead of the pump, which reduces the influence of FCA. Here, the seed is always set 1 ps ahead of the pump, although the ideal timing moves further ahead with increasing pump power. Input noise is also included at the one-photon-per-mode level (in both seeded and unseeded simulations) for the present proof of principle, although in practice it may be higher.

Input and output spectra for three different situations are shown in Fig. 2. For waveguide 1 (larger anomalous dispersion), maximum MI gain is achieved ~3.5 THz from the pump (with 10 GW/cm^2 intensity); a weak seed pulse matching this frequency experiences significant gain, but leaves gaps in the spectrum (cf. Fig. 2(a)). Somewhat counterintuitively, these gaps can be substantially reduced by driving MI

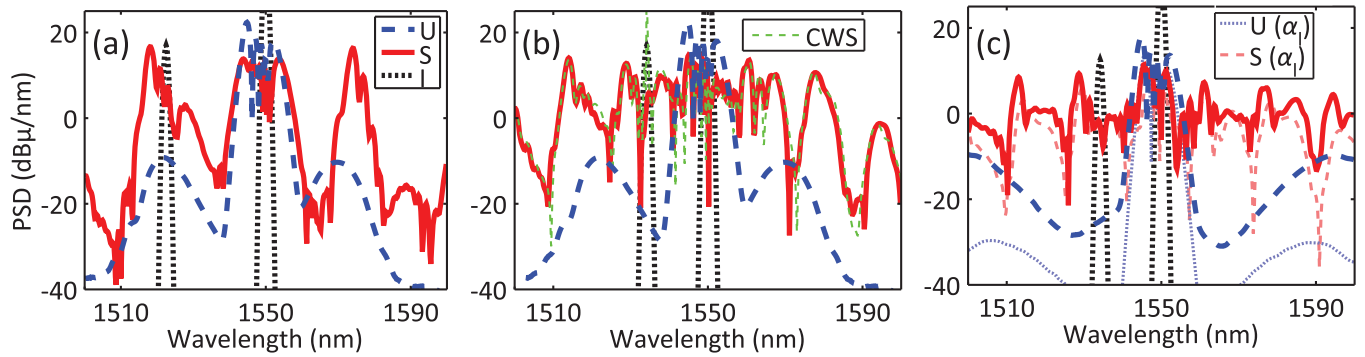

FIG. 2. (Color online) Input and output power spectral density for (a) resonant seeding in waveguide 1, (b) off-resonant seeding in waveguide 1, and (c) off-resonant seeding in waveguide 2. Unseeded (U), seeded (S), and input (I) spectra are plotted in each case. In (b), the result with quasi-continuous wave seeding (CWS) is also shown. In (c), results with linear loss $\alpha_l = 3$ dB/cm are also included. Seed shift relative to pump is 3.5 THz in (a) and 2 THz in (b) and (c). Each trace is computed from the average of 1000 independent simulations; pulse repetition rate is assumed to be 30 MHz, avoiding pulse-to-pulse carrier build-up.

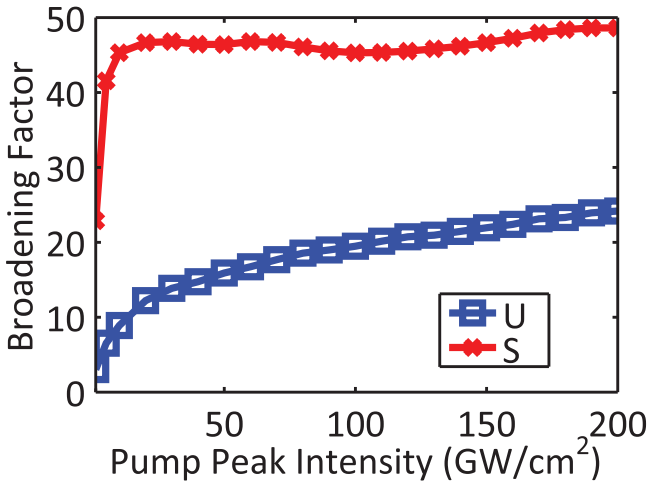

FIG. 3. (Color online) Broadening factor dependence on pump intensity with and without seeding. The broadening factor is defined as the ratio of output to input bandwidths, which are determined from the square roots of the second moments of the average output and input spectra.

off resonance with a seed at 2 THz shift (Fig. 2(b)), where the gain is smaller. The off-resonant seeding closes the gaps by pushing successive orders of MI closer to the pump, and the higher orders are closer to the gain maximum, which helps to equalize their power. This result contrasts with those of fiber-based experiments, where optimal seeding is found at or near the wavelength of maximum gain. Differences likely arise due to nonlinear losses in silicon plus the lack of broadband Raman gain. For comparison, Fig. 2(b) also shows the result with a quasi-continuous-wave seed, which yields nearly the same SC spectrum as the pulsed seed (same seed peak power).

Another example is shown in Fig. 2(c), in which reduced dispersion places the maximum of MI gain at a shift of roughly 5 THz; here, a seed shifted by 2 THz generates a SC spectrum that is even more uniform. These results indicate that seeding can be useful even when waveguides with specific dispersion profiles are not available. Fig. 2(c) also shows that the difference between the seeded and unseeded cases becomes even more significant with linear loss of $\alpha_l = 3$ dB/cm: the seeded spectrum is only slightly affected, whereas, the loss has a substantial affect on the unseeded case. Additionally, it may be noted that many of the sharp fringes in the seeded spectra result from interference and appear because of the stability of the process: they persist even when 1000 independent events are averaged together, as shown in Fig. 2. The stability enhancement is explored in further detail below. For the remainder of the paper, we focus on the waveguide with larger anomalous dispersion and fix the seed frequency shift at 2 THz, as in Fig. 2(b).

We determine the spectral broadening factor in the seeded and unseeded cases by calculating the ratio of output to input bandwidth (cf. Fig. 3). While the 20-dB bandwidth is often a useful quantity, the spectra may contain narrow depressions that produce abrupt changes in the 20-dB bandwidth as a function of, e.g., pump power. The square root of the spectrum's second moment, $\sigma_f = \sqrt{\int (f - f_1)^2 |\tilde{A}(f)|^2 df / \int |\tilde{A}(f)|^2 df}$ (centered at its weighted mean frequency, f_1) is also a measure of bandwidth, generally does not suffer from this issue, and is used here. From Fig. 3, it is clear that seeding substantially extends the broadening factor, particularly at low pump power. At such intensities, the seeded broadening factor may exceed that of the unseeded at 20-fold greater intensity. For example, broadening is 40-fold at $\sim$10 GW/cm^2 with seeding, but less than 30-fold at $\sim$200 GW/cm^2 without seeding. Thus, it becomes possible to achieve large broadening factors at intensities far below the damage threshold of the waveguides (which may be $\sim$500 GW/cm^2 or less[32]). Furthermore, nonlinear loss leads to a striking difference in efficiency: at 10 GW/cm^2, $\sim$8% of the input power remains in the output seeded SC, whereas only $\sim$0.5% remains at 200 GW/cm^2 without seeding. Clearly, a far greater fraction of the power is wasted when attempting to match the stimulated broadening factor in the unseeded case. Unseeded broadening will be accelerated with a larger amount of input noise (incoherent seeding); however, the stability advantages, which we address next, are only achieved with a coherent seed.

Fig. 4 explores the stability of seeded and unseeded spectral broadening from sets of 1000 independent trials. The signal-to-noise ratio (SNR) is determined as the mean power spectral density relative to its standard deviation at each wavelength (cf. Fig. 4(a)). As expected, the unseeded case is dominated by noise away from the SPM spectral region. With higher power, the unseeded SNR does improve slightly, but at the expense of the stability of SPM region,

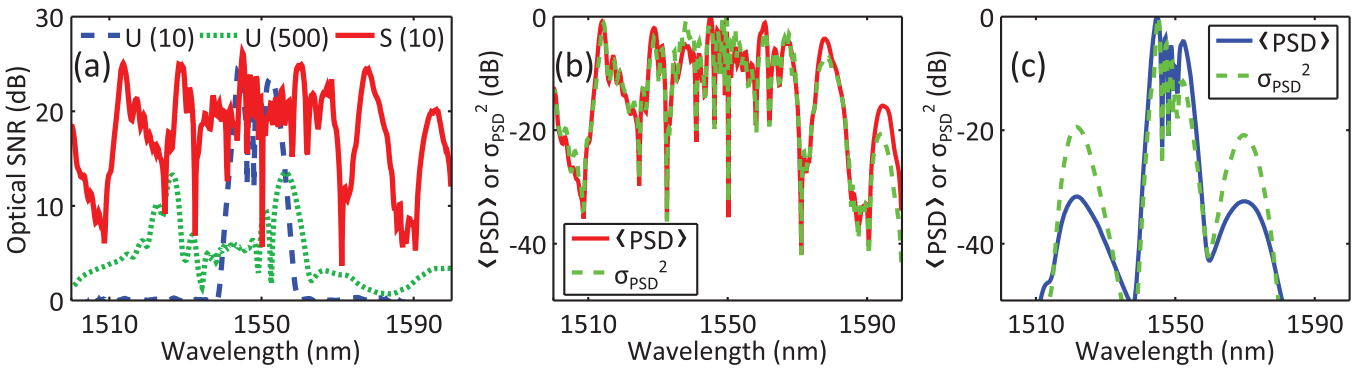

FIG. 4. (Color online) Noise properties of seeded and unseeded SC in silicon. (a) Optical signal-to-noise ratio of the seeded SC (S) at 10 GW/cm^2 and unseeded SC (U) at 10 GW/cm^2 and 500 GW/cm^2. SNRs are computed from 1000 independent events in each case. (b) Normalized mean and variance of the output spectral density for 1000 seeded events pumped at 10 GW/cm^2. (c) Same as (b) but without seeding.

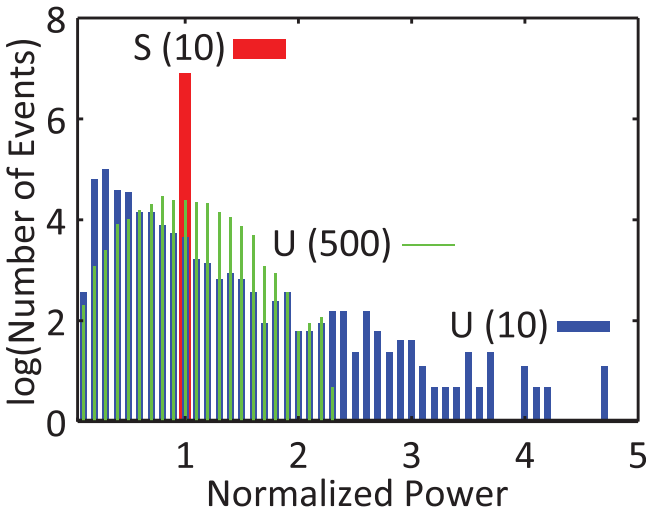

FIG. 5. (Color online) Normalized power statistics of seeded and unseeded spectra for a 10 nm bandwidth centered at 1590 nm. Histograms are normalized by their respective means to illustrate their signal-to-noise levels. Pump intensities: 10 GW/cm^2 for seeded (S) and 10 GW/cm^2 and 500 GW/cm^2 for unseeded (U).

which decreases due to depletion by the fluctuating MI. On the other hand, the SNR with seeding is dramatically improved, aside from the points of low power spectral density. In the context of amplitude modulation (on-off keying) for digital communications, an SNR of 12 dB yields a bit-error rate of 10^{-12}, indicating that seeded SC could be feasible for future WDM systems.[33]

The amount of excess noise can also be seen by comparing the average power spectral density with the variance at each wavelength (cf. Figs. 4(b) and 4(c)). Because the input noise is added to the initial field, the mean and variance of the spectral ensemble are related by a uniform factor at the input. Because of the nonlinearity, this relationship may be distorted, resulting in excess noise at the output. In the seeded case, the proportionality between mean and variance is preserved, but not in the unseeded case. For high pump power, the seeded SNR ultimately begins to decrease as the input noise has a greater influence on broadening.[22,23] Finally, the complex noise properties of the unseeded SC are further evidenced by an examination of the spectral statistics at a fixed wavelength (cf. Fig. 5). Here, we find that the fluctuations in the unseeded spectrum are distributed in a heavy-tailed fashion, reminiscent of the L-shaped distributions described above in the context of optical rogue waves from fiber-based SC generation.[21] The seeded case, which is far more stable, is also shown for comparison.

In summary, we have investigated the application of stimulated supercontinuum generation in silicon waveguides as a means of overcoming limitations from nonlinear absorption and achieving stable spectral broadening. The results of our simulations demonstrate substantial benefits from seeding—including reduced pump power requirements, improved efficiency, and much greater stability—with parameters that are experimentally realistic. We have also shown that tuning the properties of the stimulus can be used to actively control the SC spectral profile, suggesting applications in on-chip signal processing and sensing for this source of coherent light.

[1]R. Alfano, Sci. Am. **295**, 86 (2006).
[2]J. M. Dudley, G. Genty, and S. Coen, Rev. Mod. Phys. **78**, 1135 (2006).
[3]T. Udem, R. Holzwarth, and T. W. Hänsch, Nature **416**, 233 (2002).
[4]S. A. Diddams, L. Hollberg, and V. Mbele, Nature **445**, 627 (2007).
[5]P. V. Kelkar, F. Coppinger, A. S. Bhushan, and B. Jalali, Electron. Lett. **35**, 1661 (1999).
[6]N. Nishizawa, Y. Chen, P. Hsiung, E. P. Ippen, and J. G. Fujimoto, Opt. Lett. **29**, 2846 (2004).
[7]H. Kano and H. Hamaguchi, Opt. Express **13**, 1322 (2005).
[8]M. Kobrinsky, B. A. Block, J.-F. Zheng, B. C. Barnett, E. Mohammed, M. Reshotko, F. Robertson, S. List, I. Young, and K. Cadien, Intel Technol. J. **8**, 129 (2004).
[9]E. A. De Souza, M. C. Nuss, W. H. Knox, and D. A. B. Miller, Opt. Lett. **20**, 1166 (1995).
[10]S. V. Smirnov, J. D. Ania-Castanon, T. J. Ellingham, S. M. Kobtsev, S. Kukarin, and S. K. Turitsyn, Opt. Fiber Technol. **12**, 122 (2006).
[11]Ö. Boyraz, P. Koonath, V. Raghunathan, and B. Jalali, Opt. Express **12**, 4094 (2004).
[12]E. Dulkeith, Y. A. Vlasov, X. Chen, N. C. Panoiu, and R. M. Osgood, Jr., Opt. Express **14**, 5524 (2006).
[13]L. Yin, Q. Lin, and G. P. Agrawal, Opt. Lett. **32**, 391 (2007).
[14]P. Koonath, D. R. Solli, and B. Jalali, Appl. Phys. Lett. **93**, 091114 (2008).
[15]D. A. B. Miller, Proc. IEEE **88**, 728 (2000).
[16]P. Koonath, D. R. Solli, and B. Jalali, Appl. Phys. Lett. **91**, 061111 (2007).
[17]L. Yin and G. P. Agrawal, Opt. Lett. **32**, 2031 (2007).
[18]I.-W. Hsieh, X. Chen, X. Liu, J. I. Dadap, N. C. Panoiu, C.-Y. Chou, F. Xia, W. M. Green, Y. A. Vlasov, and R. M. Osgood, Jr., Opt. Express **15**, 15242 (2007).
[19]N. C. Panoiu, X. Chen, and R. M. Osgood, Jr., Opt. Lett. **31**, 3609 (2006).
[20]X. Liu, R. M. Osgood, Jr., Y. A. Vlasov, and W. M. J. Green, Nat. Photonics **4**, 557 (2010).
[21]D. R. Solli, C. Ropers, P. Koonath, and B. Jalali, Nature **450**, 1054 (2007).
[22]D. R. Solli, C. Ropers, and B. Jalali, Phys. Rev. Lett. **101**, 233902 (2008).
[23]D. R. Solli, B. Jalali, and C. Ropers, Phys. Rev. Lett. **105**, 233902 (2010).
[24]D. R. Solli, C. Ropers, and B. Jalali, Appl. Phys. Lett. **96**, 151108 (2010).
[25]J. M. Dudley, G. Genty, and B. J. Eggleton, Opt. Express **16**, 3644 (2008).
[26]A. Efimov and A. J. Taylor, Opt. Express **16**, 5942 (2008).
[27]G. Genty, J. M. Dudley, and B. J. Eggleton, J. Appl. Phys. B **94**, 187 (2009).
[28]K. K. Y. Cheung, C. Zhang, Y. Zhou, K. K. Y. Wong, and K. K. Tsia, Opt. Lett. **36**, 160 (2011).
[29]B. Kuyken, X. Liu, R. M. Osgood, Jr., R. Baets, G. Roelkens, and W. M. J. Green, Opt. Express **19**, 20172 (2011).
[30]R. A. Soref and B. R. Bennet, IEEE J. Quantum Electron. **23**, 123 (1987).
[31]M. A. Foster, A. C. Turner, J. E. Sharping, B. S. Schmidt, M. Lipson, and A. L. Gaeta, Nature **441**, 960 (2006).
[32]P. P. Pronko, P. A. VanRompay, C. Horvath, F. Loesel, T. Juhasz, X. Liu, and G. Mourou, Phys. Rev. B **58**, 2387 (1998).
[33]G. P. Agrawal, *Fiber-Optic Communication Systems*, 4th ed. (Wiley, Hoboken, New Jersey, 2010).